



**SPE-169076-MS**

## **Modeling of Viscous Displacement in Dual-Porosity Naturally Fractured Reservoirs: Application to Surfactant Enhanced Oil Recovery**

Mojtaba Kiani, Tiorco; Baharak B. Alamdari, Tiorco; Hossein Kazemi, Colorado School of Mines

Copyright 2014, Society of Petroleum Engineers

This paper was prepared for presentation at the SPE Improved Oil Recovery Symposium held in Tulsa, Oklahoma, USA, 12–16 April 2014.

This paper was selected for presentation by an SPE program committee following review of information contained in an abstract submitted by the author(s). Contents of the paper have not been reviewed by the Society of Petroleum Engineers and are subject to correction by the author(s). The material does not necessarily reflect any position of the Society of Petroleum Engineers, its officers, or members. Electronic reproduction, distribution, or storage of any part of this paper without the written consent of the Society of Petroleum Engineers is prohibited. Permission to reproduce in print is restricted to an abstract of not more than 300 words; illustrations may not be copied. The abstract must contain conspicuous acknowledgment of SPE copyright.

### **Abstract**

Surfactant-enhanced oil recovery (EOR) in fracture-dominated naturally fractured reservoirs (NFR) and very low-permeability Bakken type reservoirs is less known. Therefore, to predict its performance, improvement of the reservoir simulation tools is necessary to account for the surfactant flow mechanisms as much as possible. We present an improved *dual-porosity (DP) numerical simulation model* and algorithm in which matrix-fracture fluid transfer function was enhanced by implementing a proper viscous displacement mechanism. This mechanism was added to the existed fluid expansion, gravity drainage, and capillary pressure mechanisms. Current DP reservoir simulators generally do not account for the viscous displacement mechanism. To validate both the accuracy and efficacy of the improved model, results were compared with the results from a variable permeability-porosity, single-continuum, fine-grid model.

Simulation results of improved model were in agreement with the results of the fine-grid model as the reference case. In a one-dimensional numerical model, water flood cumulative oil production increased about 5% compared to the conventional DP model. Also, incremental oil production increased over 5% for 1 to 2 wt% surfactant concentrations. Similar results were obtained in multi-dimensional numerical models. In a representative matrix block, the water flood oil production rate started at 0.25 bbl/day in improved model compared to 0.053 bbl/day in conventional DP model. This rate was 0.124 bbl/day versus 0.03 bbl/day at the start of chemical injection. The improved model is computationally very efficient and is much faster than the fine-grid model.

For a practical application, the *improved model* was used to design and assess the viability of an EOR pilot-test using a single-well, multiple-completion protocol in a fractured carbonate reservoir. This reservoir has a matrix permeability of 10 md and matrix porosity of 0.05, and fracture permeability of 10,000 md. Similar result was obtained using improved and fine-grid models. Also sensitivity analysis was performed on fracture spacing of 5 to 20 ft. We found that smaller matrix blocks are affected more by viscous displacement.

### **Introduction**

In a DP NFR, fracture medium consists of the interconnected high-permeability cracks, but its pore space is a small fraction of the total pore space of the reservoir. Oil recovery from these reservoirs on the average is lower than sandstone reservoirs because NFRs are typically either oil-wet or mixed-wet. Wettability of carbonate reservoirs probably is the most important oil recovery controlling parameter (Austad and Milner, 1997; Morrow and Mason, 2001; Tong et al., 2002; Hirasaki and Zhang, 2006; Gupta and Mohanty, 2008). Gas and water injection has been used to improve oil production from the matrix mainly by gravity drainage (Firoozabadi et al., 1992; Pow et al., 1997; Lange, 1998; Firoozabadi, 2000; Holditch, 2006; Eggermann et al., 2007; Lemonnier and Bourbiaux, 2010). Several papers have reported chemical EOR field pilot tests: Lagomar Field, Venezuela (Manrique et al., 2000), Angsi Field, Malaysia (Othman et al., 2007), Yates Field, USA (Yang and Wadleigh, 2000; Chen et al., 2000 and 2001). Kiani et al. in 2011 provide a detailed report of the chemical EOR history in NFR.

In the NFR, viscous displacement is significant in fractures but minimal in the matrix. In chemical flooding, surfactant could partially penetrate the matrix from fractures with assistance from a secondary viscous displacement across the matrix to mobilize additional oil. Field observations and reservoir modeling support this assertion; nonetheless, there are exceptions. For instance, viscous displacement by water and gas flooding is significant in the fracture-vug-dominated Cantarell field in Gulf of Mexico.

Viscous displacement formulation in DP reservoir models is mathematically consistent with physics of flow as long as time-step sizes are large enough to establish pseudo-steady flow within each time step. This is the case when matrix permeability

is large and matrix dimensions are small enough to meet the pseudo-steady flow requirements in each time step. This condition is generally met in most conventional reservoirs, but it is not met in low-permeability unconventional oil reservoirs such as Bakken in North America. In this paper, we present a new viscous displacement algorithm, which adheres to physics of flow and is an improvement over existing methods.

The Warren and Root (1963) single-phase version of DP model has the following form:

$$\left[ \nabla \cdot \frac{k_{f,eff}}{\mu} \nabla P_f \right] - \sigma \frac{k_m}{\mu} (P_f - P_m) + \hat{q} = \phi_f c_f \frac{\partial P_f}{\partial t} \quad (1)$$

$$\sigma \frac{k_m}{\mu} (P_f - P_m) = \phi_m c_m \frac{\partial P_m}{\partial t} \quad (2)$$

In Eq.(1), the fracture flow equation differs from the original Warren-Root model because of the use of effective fracture permeability ( $k_{f,eff}$ ) instead of absolute fracture permeability ( $k_f$ ). Eq.(2), the matrix flow equation, is a resistance-capacitance (RC) formulation, which accounts only for the flow resulting from fluid expansion or compression, and is applicable to situations where pseudo-steady state approximation prevails. In reality a global coordinate system supports Eq.(1), while a local coordinate supports Eq.(2). Kazemi, et al, 1976, and Gilman and Kazemi, 1988, reported gravity and capillary force formulation for the two-phase flow in the fracture and matrix. Similarly, Ramirez et al., 2009 and Alkobaisi et al., 2009 presented three-phase flow formulations for steady state and unsteady state fluid transfer between fracture and matrix.

## 1. Dual-porosity Model without viscous displacement inside the matrix

### 1.1. Water Phase

In the absence of free gas, the following formulation is applicable and the continuity equation for water phase in fracture is:

$$\nabla \cdot \left[ \frac{(k_{f,eff} \lambda_{wf})}{B_{wf}} \right] \left[ \nabla P_{of} - \gamma_w \nabla D - \nabla P_{cwof} \right] - \tau_w + \hat{q}_{wf} = \phi_f \left[ S_{wf} (c_\phi + c_w) \frac{\partial P_{of}}{\partial t} + \frac{\partial S_{wf}}{\partial t} \right] \quad (3)$$

Where

$$\tau_w = 0.006328 \sigma \frac{k_m \lambda_{wf} / m}{B_{wf} / m} \left[ (P_{of} - P_{om}) + \frac{\sigma_z}{\sigma} \gamma_w (h_{wf} - h_{wm}) - (P_{cwof} - P_{cwom}) \right] \quad (4)$$

Eq. (4) represents the transfer function equation for water phase between fracture and matrix. Transfer function is defined as the flow rate [volume/time] per unit of rock volume, which becomes [1/time]. Terms inside the parenthesis account for fluid expansion and compression,  $(P_{of} - P_{om})$ , gravity,  $\frac{\sigma_z}{\sigma} \gamma_w (h_{wf} - h_{wm})$ , and capillary forces,  $(P_{cwof} - P_{cwom})$ , in the matrix blocks. Fluid expansion/compression term in multi-phase flow is generally negligible. The capillary and gravity forces can work together or can be against each other. Depending on the flowing phase present, capillary and gravity forces are generally dominant in fractured reservoirs. The effects of these two forces are different case to case. They can work together or can oppose each other. For example in gas injection always gravity difference will play the major role but in water flooding both mechanisms might be effective. When fluid expansion is negligible, capillary and gravity forces are dominant in the matrix, which leads the Eq. (5):

$$\tau_w = 0.006328 \sigma k_m \frac{\lambda_{wf} / m \lambda_{of} / m}{\lambda_t} \left[ (P_{cwof} - P_{cwom}) + \frac{\sigma_z}{\sigma} (\gamma_w - \gamma_o) (h_{wf} - h_{wm}) \right] \quad (5)$$

The relative effect of gravity to capillary is shown by the relative magnitude of the gravity term  $\frac{\sigma_z}{\sigma} (\gamma_w - \gamma_o) (h_{wf} - h_{wm})$  versus capillary term,  $(P_{cwom} - P_{cwof})$ . For example, if the gravity term is 1 psi and capillary term is 2 psi, for a water-wet system, then the gravity and capillary add to 3 psi, and capillary is more important than gravity. However, for an oil-wet system with -2 psi capillary term, the combined effect of capillary and gravity is -1 psi; this means that water cannot enter the matrix.

A credible transfer function accurately accounts for the matrix-fracture fluid exchange through the above mentioned forces. An accurate calculation of transfer function has a very important effect on the economics of the project. Because based on that one can determine how much of hydrocarbon in place in a NFR can be produced. **Figure 1** helps to explain the terms

used in the transfer function equation by considering a fractured rock in reservoir condition including three phases (This picture is an ideal case and is just for purpose of showing the fluid levels in the fracture and matrix block). **Figure 1** shows the water, oil, and gas levels (heads) in matrix and fractures in reservoir conditions. In **Figure 1**, the gas or water column in fractures needs to be big enough to overcome the entry capillary pressure (threshold gas or water-oil capillary pressure) of the matrix. For example in a pressure maintenance gas injection project, gas head could be more than several feet to enable the gas penetrate into the matrix. Similarly, in water flooding projects the same mechanism is involved.

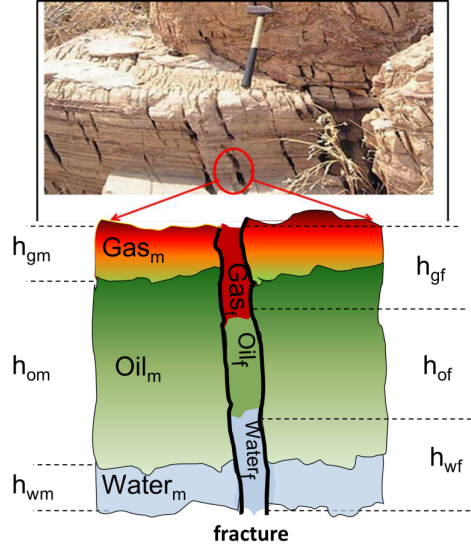


**Figure 1: Top: outcrop of fractured carbonate rock (Scott, 2008); Bottom: Schematic of fluid heads in a DP model (f:fracture, m:matrix, h:fluid head(level))**

Continuity equation for water phase in matrix is as following:

$$\tau_w = \frac{\partial}{\partial t} \left( \phi_m \frac{S_{wm}}{B_{wm}} \right) \quad (6)$$

Eq. (6) can be written in below form:

$$\tau_w = \phi_m S_{wm} (c_{\phi m} + c_w) \frac{\partial P_{wm}}{\partial t} + \phi_m \frac{\partial S_{wm}}{\partial t} \quad (7)$$

## 1.2. Oil Phase

Fracture material balances for oil phase is:

$$\nabla \cdot \left[ \frac{(k_{f,eff} \lambda_{of})}{B_{of}} \right] [\nabla P_{of} - \gamma_o \nabla D] - \tau_o + \hat{q}_{of} = \phi_f \left[ S_{of} (c_{\phi} + c_o) \frac{\partial P_{of}}{\partial t} + \frac{\partial S_{of}}{\partial t} \right] \quad (8)$$

where

$$\tau_o = 0.006328 \sigma \frac{k_m \lambda_{om/f}}{B_{om/f}} \left[ (P_{of} - P_{om}) + \frac{\sigma z}{\sigma} \gamma_o [(h_{wf} - h_{wm}) - (h_{gf} - h_{gm})] \right] \quad (9)$$

And matrix material balance (transfer function) is as following:

$$\tau_o = \frac{\partial}{\partial t} \left( \phi_m \frac{S_{om}}{B_{om}} \right) \quad (10)$$

Eq. (10) can be written in below form:

$$\tau_o = \phi_m S_{om} (c_{\phi m} + c_o) \frac{\partial P_{om}}{\partial t} + \phi_m \frac{\partial S_{om}}{\partial t} \quad (11)$$

Under a counter-current flow mechanism the amount of water transferred into the matrix is equal to the amount of oil expelled from the matrix; therefore we have:

$$\tau_o = -\tau_w \quad (12)$$

For a system including water and oil phases, by adding the fracture water and oil material balances, the form of global pressure equation becomes:

$$\nabla \cdot (k_{f,eff}) \left[ \lambda_{yf} \nabla P_{of} - (\gamma_w \lambda_{wf} + \gamma_o \lambda_{of}) \nabla D - \lambda_{wf} \nabla P_{cwof} \right] - \tau_t + \hat{q}_{yf} = \phi_f c_{yf} \frac{\partial P_{of}}{\partial t} \quad (13)$$

Eq.(13) is non-linear and in order to solve it as a set of linearized equations an approximate form has to be written in finite difference.  $\tau_t$  is total transfer function of the phases and is the sum of  $\tau_o$  and  $\tau_w$ . Solving the finite difference expansion of the above equation implicitly for pressure, the results can be used sequentially in the saturation equations to solve for the phase saturations. Then matrix phase saturation values can be obtained from Eq. (7) and Eq. (11) for water and oil respectively.

### 1.3. Fracture Surfactant Material Balance

Surfactant concentration per time step can be solved explicitly or implicitly using the finite-difference form of Eq. (14). In this equation pressures and saturations have already been calculated using Eq.(13), (7) or (11) at n+1 level. This equation includes diffusion mass transfer term, surfactant partition in oil phase, and surfactant adsorption on the rock surface.  $C_{osf/m} = \beta C_{wsf/m}$  accounts for surfactant partition into oil phase. Langmuir isotherm adsorption equation was used.

$$\begin{aligned} & \nabla \cdot \left[ \frac{k_{f,eff} \lambda_{wf}}{B_{wf}} C_{wsf} (\nabla P_{wf} - \gamma_w \nabla D) + \frac{k_{f,eff} \lambda_{of}}{B_{of}} C_{wsf} (\nabla P_{of} - \gamma_o \nabla D) \right] - (\tau_w C_{wsf/m} - \tau_o C_{osf/m}) \\ & - \nabla \cdot \left[ \left( \frac{\hat{D}}{\tau} \phi S_w \right)_m \nabla C_{wsm} \right] - \nabla \cdot \left[ \left( \frac{\hat{D}}{\tau} \phi S_o \right)_m \nabla C_{osm} \right] + \left( C_{wsf} \hat{q}_{wf} + C_{osf} \hat{q}_{of} \right) = \frac{\partial}{\partial t} \left[ \phi_f \left( C_{wsf} \frac{S_{wf}}{B_{wf}} + C_{osf} \frac{S_{of}}{B_{of}} \right) + (1 - \phi_f) \cdot \rho_r \cdot a_{sf} \right] \end{aligned} \quad (14)$$

### 1.4. Matrix Surfactant Material Balance

Eq.(15) accounts for surfactant penetration into matrix. Upstream weighting determines whether surfactant goes in or out of matrix grid block. Surfactant adsorption is included on the right hand side of Eq.(15).

$$\tau_w C_{wsf/m} - \tau_o C_{osf/m} = \frac{\partial}{\partial t} \left[ \phi_m \left( C_{wsm} \frac{S_{wm}}{B_{wm}} + C_{osm} \frac{S_{om}}{B_{om}} \right) + (1 - \phi_m) \cdot \rho_r \cdot a_{sm} \right] \quad (15)$$

Surfactant incremental oil recovery is investigated by using interfacial tension reduction and wettability alteration. The auxiliary equations for solving the pressure and saturations are given in Appendix A.

## 2. Dual-porosity Model with Viscous Displacement in the Matrix

In contrast with conventional single-porosity formulations, fluid exchange between fracture and matrix in a DP model is a replacement process rather than a displacement. To include fluid displacement in DP models viscous displacement term needs to be added. The need for implementation of the viscous displacement term was recognized by Gilman and Kazemi in 1988 and an algorithm was provided. In what follows, we have followed this early idea and have developed an easily implementable method to account for viscous displacement. **Figure 2** shows the comparison between the DP model with viscous displacement and the DP model without viscous displacement. As seen from this figure in the new work we account for the pressure gradient between fracture and matrix within the numerical grid block. In both works the matrix blocks in a given numerical grid block behaves identically. Depend on the capillary pressure insid the matrix block oil pressure can be greater than water pressure or vice versa. Assuming capillary pressure near zero in fractures, both water and oil pressures are the same. When the pressure gradient across the matrix block, in each direction, becomes larger than the capillary pressure inside the matrix, fracture fluid will flow from upstream face and matrix fluid will drop from downstream face. Viscosu

displacement mechanism was adjusted into the current DP formulation as a part of matrix-fracture transfer function terms. We have made this adjustment in the following procedure:

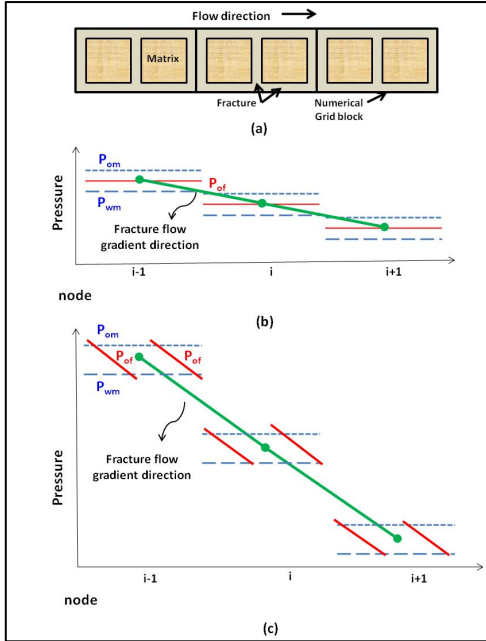


Figure 2: DP model (a) Flow into a numerical grid block with more than one matrix block (b) without viscous displacement (c) with viscous displacement (modified from Gilman and Kazemi, 1988).

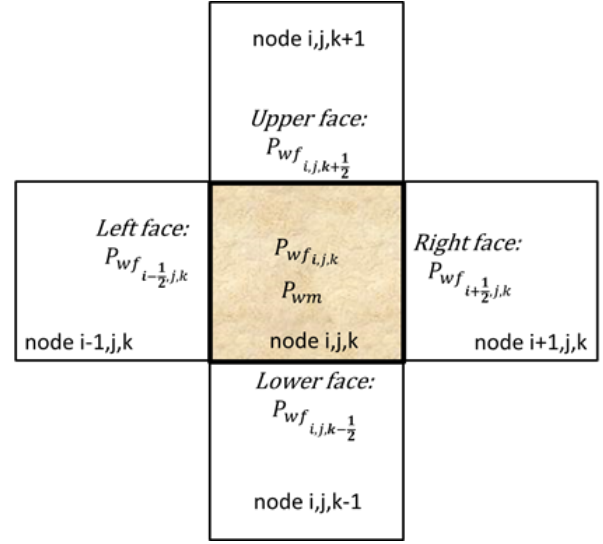


Figure 3: Schematic of a 5-point fracture-matrix grid designation and pressure nomenclature for Calculating viscous displacement in the central matrix block.

## 2.1. Adjustment inside the Fracture

The viscous displacement terms for matrix flow are represented by  $t_{w,vd}$  and  $t_{o,vd}$  for water and oil respectively. Consequently Eq.(3) becomes Eq.(16).

$$\nabla \cdot \left( \frac{k_{f,eff} \lambda_{wf}}{B_{wf}} \right) \left[ \nabla P_{of} - \gamma_w \nabla D - \nabla P_{cwof} \right] - \tau_w - \tau_{w,vd} + \hat{q}_{wf} = \phi_f \left[ S_{wf} (c_\phi + c_w) \frac{\partial P_{of}}{\partial t} + \frac{\partial S_{wf}}{\partial t} \right] \quad (16)$$

Eq. (8) becomes Eq.(17)

$$\nabla \cdot \left( \frac{k_{f,eff} \lambda_{of}}{B_{of}} \right) \left[ \nabla P_{of} - \gamma_o \nabla D \right] - \tau_o - \tau_{o,vd} + \hat{q}_{of} = \phi_f \left[ S_{of} (c_\phi + c_o) \frac{\partial P_{of}}{\partial t} + \frac{\partial S_{of}}{\partial t} \right] \quad (17)$$

In the global pressure equation, Eq.(13), the total transfer function,  $\tau_t$ , becomes:

$$\tau_t = \tau_w + \tau_o + \tau_{w,vd} + \tau_{o,vd} \quad (18)$$

In the above equations viscous displacement terms can be shown to be:

$$\tau_{w,vd} = -\vec{v}_{im} \nabla f_w \quad (19)$$

$$\tau_{o,vd} = -\vec{v}_{im} \nabla f_o \quad (20)$$

The  $\vec{v}_{im}$  is the total phase velocity vector in matrix and  $\nabla f$  is the gradient of phase fractional flow.

$$\vec{v}_{tm} = \vec{v}_{wm} + \vec{v}_{om} \quad (21)$$

Therefore the material balance equation for each phase in a matrix block becomes:

$$\tau_w - \vec{v}_{tm} \nabla f_w = \phi_m \frac{\partial S_{wm}}{\partial t} \quad (22)$$

$$\tau_o - \vec{v}_{tm} \nabla f_o = \phi_m \frac{\partial S_{om}}{\partial t} \quad (23)$$

Integrating Eq.(22) or Eq.(23) with respect to the volume of the matrix block:

$$\int_{V_m} \tau_w - \int_{V_m} \vec{v}_{tm} \nabla f_w dv = \int_{V_m} \phi_m \frac{\partial S_{wm}}{\partial t} dv \quad (24)$$

Where the volume of matrix block is:

$$V_m = l_x l_y l_z \quad (25)$$

$$\int_{V_m} \tau_w - \int \left( v_{imx} \frac{\partial f_w}{\partial x} + v_{imy} \frac{\partial f_w}{\partial y} + v_{imz} \frac{\partial f_w}{\partial z} \right) dx dy dz = V_m \phi_m \frac{\partial S_{wm}}{\partial t} \quad (26)$$

$$\int_{V_m} \tau_w - v_{imx} \int \left( \frac{\partial f_w}{\partial x} \right)^{ups} dy dz - v_{imy} \int \left( \frac{\partial f_w}{\partial y} \right)^{ups} dx dz - v_{imz} \int \left( \frac{\partial f_w}{\partial z} \right)^{ups} dx dy = V_m \phi_m \frac{\partial S_{wm}}{\partial t} \quad (27)$$

For a two dimensional vertical model:

If  $v_{imx} > 0$  and  $v_{imz} > 0$ , then

$$\tau_w V_m - v_{imx} l_y l_z (f_{wm} - f_{wf}) - v_{imz} l_y l_x (f_{wm} - f_{wf}) = V_m \phi_m \frac{\partial S_{wm}}{\partial t} \quad (28)$$

Otherwise

$$\tau_w V_m - v_{imx} l_y l_z (f_{wf} - f_{wm}) - v_{imz} l_y l_x (f_{wf} - f_{wm}) = V_m \phi_m \frac{\partial S_{wm}}{\partial t} \quad (29)$$

Then Eq.(28) becomes:

$$\tau_w - v_{imx} \frac{f_{wm} - f_{wf}}{l_x} - v_{imz} \frac{f_{wm} - f_{wf}}{l_z} = \phi_m \frac{\partial S_{wm}}{\partial t} \quad (30)$$

And Eq.(29) becomes:

$$\tau_w - v_{imx} \frac{f_{wf} - f_{wm}}{l_x} - v_{imz} \frac{f_{wf} - f_{wm}}{l_z} = \phi_m \frac{\partial S_{wm}}{\partial t} \quad (31)$$

The similar approach for the oil phase is given below:

If  $v_{imx} > 0$  and  $v_{imz} > 0$

$$\tau_o - v_{imx} \frac{f_{om} - f_{of}}{l_x} - v_{imz} \frac{f_{om} - f_{of}}{l_z} = \phi_m \frac{\partial S_{om}}{\partial t} \quad (32)$$

Otherwise

$$\tau_o - v_{imx} \frac{f_{of} - f_{om}}{l_x} - v_{imz} \frac{f_{of} - f_{om}}{l_z} = \phi_m \frac{\partial S_{om}}{\partial t} \quad (33)$$

The viscous displacement velocity affecting a matrix block for each phase is:

$$\vec{v}_{wm} = -0.006328k_m \lambda_{wm} \left( \nabla P_w^{(n+1)} - \gamma_w \nabla D \right) \quad (34)$$

And

$$\vec{v}_{om} = -0.006328k_m \lambda_{om} \left( \nabla P_o^{(n+1)} - \gamma_o \nabla D \right) \quad (35)$$

The sum of Eq.(34) and Eq.(35) results Eq.(21).

For a matrix block with four faces in x-z plane shown in **Figure 3**, the discretized form of the above phases velocities are:

$$v_{\varphi mx} = -0.006328k_m \lambda_{\varphi m} \left( \frac{P_{\varphi f_{i+\frac{1}{2}}}^{n+1} - P_{\varphi f_{i-\frac{1}{2}}}^{n+1}}{\Delta x} - \gamma_{\varphi} \frac{D_{i+\frac{1}{2}}^n - D_{i-\frac{1}{2}}^n}{\Delta x} \right) \quad (36)$$

$$v_{\varphi mz} = -0.006328k_m \lambda_{\varphi m} \left( \frac{P_{\varphi f_{k+\frac{1}{2}}}^{n+1} - P_{\varphi f_{k-\frac{1}{2}}}^{n+1}}{\Delta z} - \gamma_{\varphi} \frac{D_{k+\frac{1}{2}}^n - D_{k-\frac{1}{2}}^n}{\Delta z} \right) \quad (37)$$

In the above equations:

The pressure at each face, left (-) and right (+), of the matrix block is given by:

$$P_{i\pm\frac{1}{2}} = \left( 1 + \frac{k_i}{k_{i\pm 1}} \frac{\Delta x_{i\pm 1}}{\Delta x_i} \right)^{-1} P_{i\pm 1} + \left( 1 + \frac{k_{i\pm 1}}{k_i} \frac{\Delta x_i}{\Delta x_{i\pm 1}} \right)^{-1} P_i \quad (38)$$

Similar equations apply to y and z directions. For a model with uniform grid and constant fracture permeability the above equations become:

Pressure at the right face of matrix block for each phase

$$P_{\varphi f_{i+\frac{1}{2}}}^{n+1} = \frac{P_{\varphi f_{i+1}}^{n+1} + P_{\varphi f_i}^{n+1}}{2} \quad (39)$$

Pressure at the left face of matrix block for each phase

$$P_{\varphi f_{i-\frac{1}{2}}}^{n+1} = \frac{P_i^{n+1} + P_{i-1}^{n+1}}{2} \quad (40)$$

Pressure at the top face of matrix block for each phase

$$P_{\varphi f_{k+\frac{1}{2}}}^{n+1} = \frac{P_{k+1}^{n+1} + P_k^{n+1}}{2} \quad (41)$$

Pressure at the bottom face of matrix block for each phase

$$P_{\varphi f_{k-\frac{1}{2}}}^{n+1} = \frac{P_k^{n+1} + P_{k-1}^{n+1}}{2} \quad (42)$$

Similar equations was applied during chemical injection.

### 3. Conceptual Examples

In below examples (**Table 1**) we showed the results of using the DP model with and without viscous displacement in a waterflood scenario which was followed by a surfactant flood. Results were compared with variable permeability-porosity model (fine-grid model) as the reference. The properties of these examples are given in **Table 2**.

**Table 1: Conceptual model examples**

Example	DP With Viscous Displacement	DP Without Viscous Displacement	Variable Permeability-Porosity fine-grid	Dimension	Alignment	Size
1	YES	-	-	1D	Horizontal	12x1x1
2	-	YES	-	1D	Horizontal	12x1x1
3	-	-	YES	1D	Horizontal	25x3x3
4	YES	-	-	1D	Vertical	1x1x12
5	-	YES	-	1D	Vertical	1x1x12
6	-	-	YES	1D	Vertical	3x3x25
7	YES	-	-	3D	-	10x1x10
8	-	YES	-	3D	-	10x1x10
9*	YES	-	-	3D	-	10x1x10
10*	-	YES	-	3D	-	10x1x10
11*	-	-	YES	3D	-	21x3x21

\*: These examples have different relative permeability properties; look at **Table 2**.

**Table 2: Conceptual model properties**

Properties	Example 1 to 8		Example 9 to 11	
	Matrix	Fracture	Matrix	Fracture
Initial pressure, psia	3000	3000	3000	3000
Permeability, md	10	10000	10	10000
Porosity	0.05	0.02	0.05	0.02
Oil viscosity, cp	3	3	3	3
Water viscosity, cp	0.5	0.5	0.5	0.5
$S_{wi}$	0.25	0.02	0.25	0.02
$S_{orw}$	0.3	0.02	0.3	0.02
$n_w$	2	1.3	2	1.3
$n_{ow}$	6	1.3	4	1.3
$K_{rw}$ end point	0.05	0.98	0.25	0.98
$K_{row}$ end point	0.07	0.98	0.7	0.98

#### 3.1. Simulation results

**Figure 4** and **Figure 5** show simulation results in horizontal and vertical one dimensional model (examples 1 to 6). The result of one dimensional DP model with viscous displacement was compared with the DP model without viscous displacement. This result was also compared with the one dimensional variable permeability-porosity fine-grid model. Results showed that application of viscous displacement in the DP model improves oil production in both water flood and surfactant flood stages. Surfactant was injected after 1,000 days of water flood. Results were compared for 1 wt% (10,000



faster than the computation time of the fine-grid model. The computation time for DP model was in matter of few minutes against the hours for the fine-grid model in different scenarios. The effect of matrix block size on the DP model with viscous displacement was shown in **Figure 9**. As seen smaller matrix blocks ( $l_x=l_y=l_z=5$  ft) resulted in more oil recovery than the larger ones because the viscous displacement was more effective when the fracture spacing is small. In this case a higher pressure gradient existed around matrix block. However for matrix blocks with high thickness and smaller width the combined effect of viscosity and gravity gave higher oil recovery during surfactant injection ( $l_x=l_y=5$  ft,  $l_z=20$  ft).

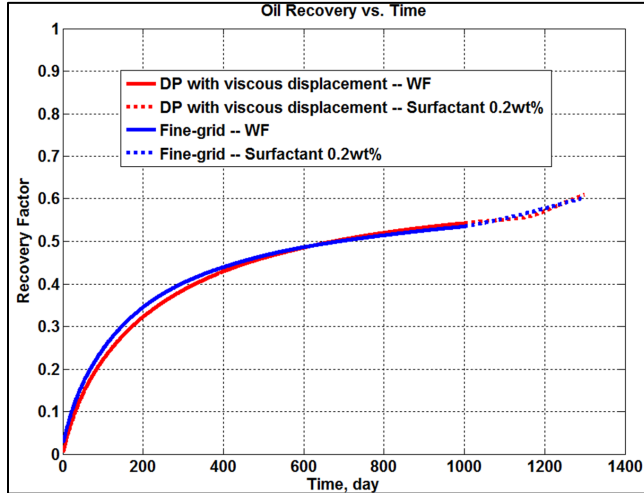


**Figure 8:** DP with viscous displacement vs. variable permeability-porosity model in a single-well dual-completion case (Example 9 and 11).

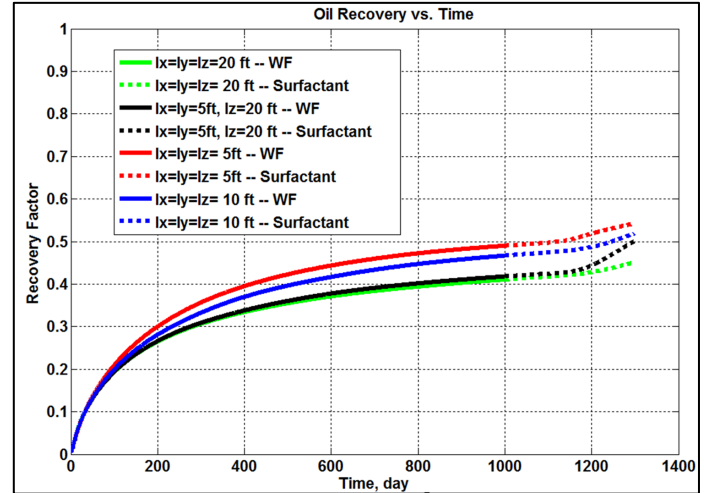


**Figure 9:** The effect different matrix block size on DP with viscous displacement effect

**Figure 10** and **Figure 11** show phase transfer function and production rate in a representative matrix block in DP model. In these figures the DP model with viscous displacement was compared with the DP model without this mechanism. As seen in **Figure 10** the transfer function for the DP model with viscous displacement was improved and more fluid can be exchanged between matrix and fracture. Due to a good fluid exchange more oil was produced in the model with viscous displacement (**Figure 11**). In water flood stage the matrix grid oil production rate started at 0.25 bbl/day in improved model compared to 0.053 bbl/day in conventional DP model. During surfactant injection even the transfer function was increased more, because more surfactant concentration could be carried into the matrix and releases more residual oil. This amount was 0.124 bbl/day against the 0.03 bbl/day at the start of chemical injection. This increases the incremental oil production during surfactant injection.

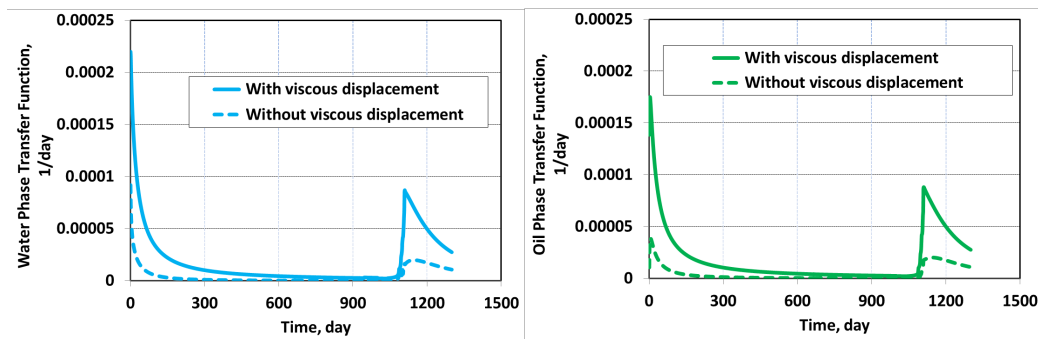


**Figure 10:** Comparison of water (left) and oil (right) transfer function in the DP model with and without viscous displacement in a representative matrix block (Example 9 and 10).

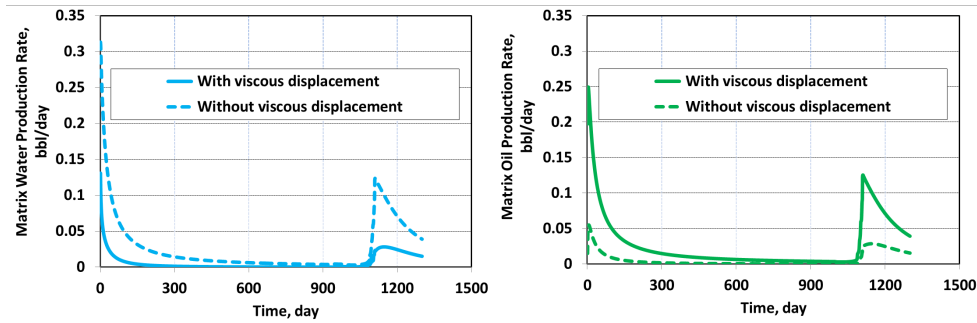


Figure 11: Comparison of water (left) and oil (right) production rate from a representative matrix block in the DP model with and without viscous displacement (Example 9 and 10).

## Discussion

The main issue with surfactant injection in carbonate NFR is shallow penetration of surfactant into the matrix. In oil-wet rocks, spontaneous capillary imbibition is absent. In fact, negative capillary pressure is present, which hinders oil drainage; however, for tall matrix blocks, there is often sufficient gravity force to push the surfactant solution into the matrix. In DP models, gravity is constrained by the matrix block height. In variable permeability-porosity fine-grid models the gravity is controlled by formation and bed thickness. Chemical injection in current DP models results in lower incremental oil compared to the fine-grid formulation, because gravity and viscous displacement forces in fine-grid models dominate the negative capillary pressures. Which model is the more reasonable one to use is a question. The oil recovery results from either model are highly subjective. But the DP results are more realistic for pattern chemical floods, because in large reservoirs the viscous displacement contribution is small in the inter-well region.

## Conclusions

As a result of this study following conclusion can be made:

1. With large pressure gradients between fracture and matrix in DP model, the viscous displacement could improve the oil displacement from the matrix. In this paper a very efficient formulation and algorithm was developed to account for viscous displacement in DP model. Simulation results of DP model including viscous displacement were verified by comparison to the variable permeability-porosity fine-grid model as the reference case.
2. Surfactant based EOR methods in DP models is more effective when viscous displacement is included.
3. In single-well dual-completion pilot test, the DP model with viscous displacement formulation is more appropriate than the DP model without this mechanism. However, viscous displacement contribution is small in the inter-well region of reservoirs with large well spacing.
4. The simulation run time for the DP model with viscous displacement algorithm is several orders of magnitude faster than the run time for the fine-grid model.

## Nomenclature

$a_s$	adsorption, mili-gram/gram rock
$B_\phi$	formation volume factor of phase $\phi$ , rb/STB
$c_t$	total system compressibility, $L^2/m$ , psi-1
$c_\phi$	compressibility of phase $\phi$ , $L^2/m$ , psi-1
$c_\phi$	pore compressibility, $L^2/m$ , psi-1
$C_{\phi s}$	Surfactant concentration in phase $\phi$ , mili-gram/gram rock
$D$	depth, ft
$\bar{D}$	diffusivity, $L^2/t$ , $ft^2/day$
$f_\phi$	fractional flow, dimensionless
$h_\phi$	gravity head for phase $\phi$ , ft
$h_f$	fracture height, L, ft
$h_{wf}$	height of water inside the fracture, ft
$h_{wm}$	height of water inside the matrix, ft
$k_{f,eff}$	effective fracture permeability, $k_{f,eff} = k_f \phi_f$
$k$	$0.006328 \times$ absolute permeability, $L^2$ , md

$k_f$	0.006328* fracture absolute permeability, $L^2$ , md
$k_{r\varphi}$	relative permeability to phase $\varphi$ , dimensionless
$L$	matrix block dimension, ft
$P_\varphi$	pressure of phase $\varphi$ , psi
$P_{cwo}$	water-oil capillary pressure, psi
$q_\varphi$	source/sink term for phase $\varphi$ , $L^3/t$ , $ft^3/d$
$\hat{q}$	sink/source term per volume of grid block, $1/t$ , $1/day$
$S_\varphi$	saturation of phase $\varphi$ , fraction
$S_{\varphi r}$	residual saturation of phase $\varphi$ , fraction
$v_\varphi$	phase velocity, ft/day
0.006328	conversion factor to the field units of psi, psi/ft, cp, ft, md, ...
<i>Greek Letters</i>	
$\tau_\varphi$	matrix / fracture transfer function for phase $\varphi$ , $1/day$
$\tilde{\tau}$	tortuosity, dimensionless
$\lambda_\varphi$	mobility of phase $\varphi$ , $cp^{-1}$
$\lambda_t$	total system mobility, $cp^{-1}$
$\Phi_m$	matrix porosity, fraction
$\Phi_f$	fracture porosity, fraction
$\gamma_\varphi$	fluid gravity gradient for phase $\varphi$ , psi/ft
$\sigma$	matrix block shape factor, $L^{-2}$ , $1/ft^2$
$\sigma_z$	matrix shape factor in z direction, $L^{-2}$ , $1/ft^2$
$\beta_s$	partition coefficient, dimensionless
$\rho_r$	rock density, $lbm/ft^3$
<i>Operators</i>	
$\nabla$	gradient operator
$\nabla \cdot$	divergence operator
<i>Superscript</i>	
$n$	current time level
$n + 1$	next time level to be solved
<i>Subscript</i>	
$m$	matrix
$f$	fracture
$o$	oil
$w$	water
$t$	total, system
$\varphi$	fluid phase ( $\varphi = o, oil$ ; $\varphi = w, water$ )

## Acknowledgement

The authors thank PEMEX for its financial support and Marathon Center of Excellence for Reservoir Studies (MCERS) at Colorado School of Mines and TIORCO for their technical support of this study.

## References

- Alkhabaisi M., Kazemi H., Ramirez B., Ozkan E., and Atan S., 2009, A critical review for proper use of water/oil/gas transfer functions in dual-porosity naturally fractured reservoirs: part II, SPE Reservoir Evaluation and Engineering
- Austad T., Milter J., 1997, Spontaneous Imbibition of Water into Low Permeable Chalk at Different Wettabilities Using Surfactants, International Symposium on Oilfield Chemistry, Houston, TX
- Chen, H. L., Lucas, L. R., Nogaret, L. A. D., Yang, H. D., Kenyon, D. E., 2001, Laboratory Monitoring of Surfactant Imbibition Using Computerized Tomography, SPE Reservoir Evaluation and Engineering, Mexico
- Egermann P., Laroche C., Manceau E., Delamaide E., Bourbiaux B., 2007, Experimental and Numerical Study of Water/Gas Imbibition Phenomena in Vuggy Carbonates, SPE Reservoir Evaluation and Engineering
- Firoozabadi A., Ottesen B., Mikklesen M., 1992, Measurements of Supersaturation and Critical Gas Saturation, SPE Formation Evaluation
- Firoozabadi A., 2000, Recovery Mechanism in Fractured Reservoirs and Field Performance, Journal of Canadian Petroleum Technology
- Gilman, J. R., Kazemi, H., 1988, Improved Calculations for Viscous and Gravity Displacement in Matrix Blocks in Dual-Porosity Simulators, SPE, Journal of Petroleum Technology
- Gupta, R., Mohanty, K. K., 2008, Wettability Alteration of Fractured Reservoirs, SPE/DOE Improved Oil Recovery Symposium, Tulsa, OK
- Hirasaki, G. and Zhang, D. L., 2004, Surface Chemistry of Oil Recovery from Fractural, Oil-Wet, Carbonate Formations, SPE Journal
- Holditch S.A., 2006, Tight Gas Sands, Journal of Petroleum Technology
- Lange E.A., 1998, Correlation and Prediction of Residual Oil Saturation for Gas-Injection Enhanced Oil-Recovery Processes, SPE Journal
- Lemonnier P., Bourbiaux B., 2010, Simulation of Naturally Fractured Reservoirs, State of the Art, Part 1, Physical Mechanism and Simulator Formulation, Oil and Gas Science and Technology, IFP
- Lemonnier P. and Bourbiaux B., 2010, "Simulation of Naturally Fractured Reservoirs, State of the Art, Part 2, Matrix-Fracture Transfers

- and Typical Features of Numerical Studies,” Oil and Gas Science and Technology, IFP
- Kazemi, H., Gilman, J.R., Elsharkawy, A.M., 1992, Analytical and Numerical Solution of Oil Recovery from Fractured Reservoirs with Empirical Transfer Functions, SPE Reservoir Engineering, SanAntonio, TX
- Kazemi, H., Merrill, L. S. Jr., Porterfield, K. L. and Zaman, P. R., 1976, Numerical Simulation of Water-Oil Flow in Naturally Fractured Reservoirs, SPE Journal
- Kiani, M., Kazemi, H., Ozkan, E., Wu, Y.S., 2011, Pilot Testing Issues of Chemical EOR in Large Fractured Carbonate Reservoirs, SPE Annual Technical Conference and Exhibition, Denver, CO.
- Manrique, E.; Carvajal, G.; Anselmi, L.; Romero, C.; Chacon, L., 2000, Alkali/Surfactant/Polymer at VLA 6/9/21 Field in Maracaibo Lake: Experimental Results and Pilot Project Design, SPE 59363, In Proceedings of SPE/DOE Improved Oil Recovery Symposium, Tulsa, OK.
- Morrow, N.R. and Mason, G., 2001, Recovery of Oil by Spontaneous Imbibition, Current Opinion in Colloid and Interface Science
- Othman, M.; Chong, M.O.; Sai, R.M.; Zainal, S.; Zakaria, M.S.; Yaacob, A.A., 2007, Meeting the Challenges in Alkaline Surfactant Pilot Project Implementation at Angsi Field, Offshore Malaysia, SPE 109033, Offshore Europe, Aberdeen, Scotland, U.K.
- Pow, M., Allan V., Mallmes R., Kantzas A., 1997, Production of Gas From Tight Naturally-Fractured Reservoirs With Active Water, Annual Technical Meeting of the Petroleum Society, Calgary, Canada
- Ramirez, B., Kazemi, H., Alkobaisi, M., and Ozkan, E., 2008, A Critical Review for Proper Use of Water/Oil/Gas Transfer Functions in Dual-Porosity Naturally Fractured Reservoirs: Part I, SPE Reservoir Evaluation and Engineering, CA.
- Scott, J; 2008, outcrop of a fractured carbonate formation, [http://www.geoexpro.com/country\\_profile/mali](http://www.geoexpro.com/country_profile/mali), Accessed October 2010
- Seethepalli, B. A., B., Mohanty K. K., 2004, Wettability Alteration during Surfactant Flooding of Carbonate Reservoirs, SPE 89423, SPE /DOE 14th Symposium on IOR, Tulsa OK
- Tong, Z. X.; Morrow, N. R. and Xie, X., 2002, Spontaneous Imbibition For Mixed-Wettability States In Sandstones Induced By Adsorption From Crude Oil, International Symposium on Reservoir Wettability, Tasmania, Australia
- Warren J.E. and Root P.J., 1963, The Behavior of Naturally Fractured Reservoirs, SPE Journal
- Xie, X., Weiss, W. W., Tong, Z., Morrow, N. R., 2004, Improved Oil Recovery from Carbonate Reservoirs by Chemical Stimulation, SPE
- Yang, H. D., and Wadleigh, E. E., 2000, Dilute Surfactant IOR-Design Improvement for Massive, Fractured Carbonate Applications, SPE 59009, SPE International Petroleum Conference and Exhibition in Mexico, Villahermosa89424, SPE/DOE 14th Symposium on IOR. Tulsa OK

## Appendix A :Auxiliary equations used in model

Shape factor for DP formulation w/o refinement:

$$\sigma = 4\left(\frac{1}{L_x^2} + \frac{1}{L_y^2} + \frac{1}{L_z^2}\right)$$

Shape factor in z direction for DP w/o refinement:

$$\sigma_z = \frac{4}{L_z^2}$$

Fluid gravity:

$$\gamma_\phi = \frac{\rho_\phi}{144}$$

Total compressibility:

$$c_t = c_\phi + S_w c_w + S_o c_o + S_g c_g$$

Water compressibility:

$$c_{wf} = -\frac{1}{B_{wf}} \frac{\partial B_{wf}}{\partial p}$$

Formation volume factor:

$$B_{wf} = B_{wfb} (1 - c_{wb} P_w)$$

Oil compressibility:

$$c_{of} = -\frac{1}{B_{of}} \frac{\partial B_{of}}{\partial P}$$

Mobility ratio:

$$\lambda_\phi = \frac{k_{r\phi}}{\mu_\phi}$$

Total mobility ratio:

$$\lambda_t = \lambda_w + \lambda_g + \lambda_o$$

Phase fractional flow:

$$f_\phi = \frac{\lambda_\phi}{\lambda_t}$$

Relative permeability:

$$k_{r\phi} = k_{r\phi}(S_w)$$

Capillary pressure:

$$P_{cow} = P_{cow}(S_w)$$

Saturation constraints:

$$S_w + S_o + S_g = 1$$

Water level (head) in matrix or fracture

$$h_{wm/f} = \left( \frac{S_{wm/f} - S_{wrm/f}}{1 - S_{wrm/f} - S_{orwm/f}} \right) L_z$$

Oil level (head) in matrix or fracture

$$h_{om/f} = \left( \frac{1 - S_{wm/f} - S_{orwm/f}}{1 - S_{wrm/f} - S_{orwm/f}} \right) L_z$$

### Relative permeability and capillary pressure equations

Water relative permeability in matrix/fracture:

$$k_{rwm/f} = k_{rwm/f}^{\max} \left( \frac{S_{wm/f} - S_{wrm/f}}{1 - S_{wrm/f} - S_{orwm/f}} \right)^{nwm/f}$$

Oil relative permeability in matrix/fracture:

$$k_{rom/f} = k_{rom/f}^{\max} \left( \frac{1 - S_{wm/f} - S_{orwm/f}}{1 - S_{wrm/f} - S_{orwm/f}} \right)^{nom/f}$$

Capillary pressure in matrix:

$$S_{wm} < S_{wrm} \quad \rightarrow P_{cwo} = 1 \text{ psi}$$

$$S_{wm} > S_{wrm} \text{ and } S_{wm} < S_{wx} \quad \rightarrow P_{cwo} = \alpha_2 \log \left( \frac{1 - S_{wx} - S_{wrm}}{S_{wm} - S_{wrm}} \right) \text{ psi}$$

$$S_{wm} > S_{wx} \text{ and } S_{wm} < 1 - S_{orwm} \quad \rightarrow P_{cwo} = \alpha_1 \log \left( \frac{1 - S_{wx} - S_{orwm}}{1 - S_{wm} - S_{orwm}} \right) \text{ psi}$$

$$S_{wm} > 1 - S_{orwm} \quad \rightarrow P_{cwo} = -8 \text{ psi}$$

where

$$\alpha_2 = - \left( \frac{S_{wx} - S_{wrm}}{1 - S_{wx} - S_{orwm}} \right) \alpha_1, \text{ and } \alpha_1 = -0.1$$

In presence of surfactant, phase relative permeability, capillary pressure, and fluid heads (level) in both matrix and fractures was calculated as a function of surfactant residual oil saturation ( $S_{orw_{m/f}}^*$ ). Therefore in above equations  $S_{orw_{m/f}}$  (water flood residual oil saturation) was replaced by  $S_{orw_{m/f}}^*$ .